TRACING AND MODELLING WATER AND SEDIMENT DYNAMICS IN A SPRINKLER IRRIGATED BED SYSTEM UNDER DIFFERENT SCENARIOS

G. Guzmán[1*], A. Laguna[2], J. C. Cañasveras[1], H. Boulal[3], H. Gómez-Macpherson[4], V. Barrón[1], J.V. Giráldez[1,4] and J. A. Gómez[4]

[1]Dept. of Agronomy, University of Córdoba, Ctra. Madrid km 396, 14071 Córdoba, Spain. e-mail: g92gudim@uco.es.
[2]Dept. of Applied Physics, University of Córdoba, Ctra. Madrid km 396, 14071 Córdoba, Spain.
[3]IPNI, North Africa, Settat Regional Center, P.O. Box 589, Settat Morocco.
[4]Institute for Sustainable Agriculture-CSIC, Alameda del Obispo, 14080 Córdoba, Spain.

RESUMEN. El uso de trazadores de sedimento ofrece un nuevo método muy eficaz para el análisis de la pérdida y redistribución de suelo en cuencas, así como para la identificación de las fuentes de sedimento. Se ha evaluado el comportamiento como trazador de sedimentos de tres óxidos de hierro en un cultivo alomado de algodón en regadío con tránsito controlado de maquinaria. Para estimar la evolución de la concentración de trazador en el suelo, se realizaron varias simulaciones de lluvia en mini parcelas. Posteriormente, con el sistema de riego por aspersión de la parcela, se comparó el sedimento generado con el estimado a través de la concentración de trazador medida y diferenciando entre surcos con y sin tránsito. Los resultados mostraron la eficacia de los tres óxidos de hierro en la identificación del origen de los sedimentos.
Se describió el flujo de agua y sedimentos con un modelo sencillo de erosión, y, con un modelo distribuido, más completo, se evaluó la influencia de varios factores ambientales.

ABSTRACT. The use of sediment tracers opens a promising way for the estimation of soil loss, redistribution and sediment yields from watersheds, identifying the sources. The performance of three iron oxides as sediment tracers has been evaluated in an irrigated ridged cotton crop plot with controlled machinery traffic. Several rainfall simulations at mini-plot scale were used, previously, to estimate the evolution of tracer concentration in the soil. Later in the sprinkler-irrigated ridged cotton crop measured sediment yields, with and without traffic, were compared with the predicted values based on tracer concentrations. Results indicate the efficiency of the method in the identification of sediment sources. All three iron oxides were useful as sediment tracers.
Water and sediment yields were described with a simple soil erosion model. A more complete distributed model was also chosen to assess the influence of some environmental factors.

1.- Introduction

Erosion is a severe environmental threat in Mediterranean landscapes due to the combination of intense showers, long dry and hot periods, which does not help to sustain a natural vegetation cover, and land steepness. In addition to these factors, weeds removal by farming practices leave a bare soil surface unprotected against the main erosion agents, water and wind.

Soil productivity loss and diffuse contamination by agrochemicals and sediment are major concerns for agricultural management of steep landscapes. The introduction of sediment tracers opens a new way to improve our understanding of erosive processes and to evaluate more precisely their effects. Many substances and soils of particular properties have been used as sediment tracers: radionuclides (*e.g.* Walling et al.1999), rare earth oxides (*e.g.* Zhang et al. 2003) or innovative tracers such as, organophilic clays (Strauss et al. 2012).

Guzmán et al. (2013) thoroughly reviewed these tracing techniques, identifying the key points and limitations of each approach, including fingerprinting studies.

Iron oxides fulfill many of the requirements defined by Zhang et al (2001), for being ideal sediment tracers. Their potential had been evaluated at laboratory scale (Guzmán et al. 2010) and at field scale (Guzmán et al. 2013) in water erosion experiments. Furthermore, iron oxides are available at a moderate price and they can be measured quickly at the laboratory or field without destructing the sample with simple equipment and relatively inexpensive.
The purpose of this report is the evaluation of three iron oxides, magnetite, hematite and goethite, as tracers in erosion trials at mini-plot and field scale to study soil erosion dynamics.

2.-Material and methods

The experimental field was located at the experimental farm Alameda del Obispo (Córdoba, Spain). The climate is Mediterranean with average annual rainfall of 600 mm. The top 10 cm of the soil profile has a 10% of clay, and 42.6% of sand. The soil belongs to the subgroup of *Typic Xerofluvents* (Soil Survey Staff, 2010).

The plot 144m long and 9 m wide, with a slope of 0.008, consisted of ten 0.25 m high ridges, 0.85 mspaced, under conventional tillage. The furrows, 0.59 m wide, acted as wheel tracks, leaving alternatively one every other traffic-free. A maize-cotton crop rotation was started in 2007. In late February 2009, crop maize residues were chopped and incorporated into the soil before forming the ridges on March 2009. Later, on May 2009, a cotton crop was sown and hand-picked on September 2009. Soil management, crop characteristics and experimental field properties are described in more detail in Boulal et al. (2011a,b; 2012).

The rainfall simulation tests were performed during 2009/2010 when cotton was established in the experimental field. A portable rainfall simulator (Alves et al. 2008) generated sixteen rain events of approximately 1.15 hours, enough to keep one hour of rainfall after runoff initiation, at an intensity of 60 mm h^{-1}. The value of rain intensity is the lower threshold of what can be considered a torrential event (Llasat, 2001).

These simulations were carried out in mini-plots of 0.81 m^2 (Fig. 1a) under different traffic conditions, furrows with (+T), and without traffic (–T), at two stages of the cotton cycle: newly formed furrows before sowing (March 2009), and with standing residues before reforming the ridgesand before chopping residues (March 2010).

The irrigation test at field scale was carried out on July 2009 using sprinklers (VYR-60) that provided 18 mm h^{-1} rate during 8.5 h. The test was done during the night to minimize wind effect, when the cotton crop covered roughly 50 % of the soil surface.

2.1.- Sediment tracers

Three different synthetic iron oxides were used as sediment tracers: magnetite (Fe_3O_4), hematite (α-Fe_2O_3) and goethite (FeOOH), commercially available as Bayferrox® 318M, 110 and 920, respectively. Their characteristics allow relatively easy detection and measurement through magnetic susceptibility in the case of magnetite, and diffuse reflectance spectroscopy for hematite and goethite.

Magnetic susceptibility was measured using a Bartington® meter and a MS2B® dual frequency sensor for laboratory measurements. For the case of hematite and goethite measurements, the total iron (Fe_d) was determined by the method of Mehra and Jackson (1960), modified by carrying out the extraction at 25 ºC for 16 h. Diffuse reflectance spectra were recorded from 300 to 2500 nm in 0.5 nm steps using a Cary 5000 UV–Vis–IR spectrophotometer (Varian Inc., Palo Alto, CA) equipped with an integrating sphere.

Before the execution of the rainfall simulation experiments, a mixture of soil and magnetite was prepared following the methodology proposed by Guzmán et al. (2010). The mixture was spread onto the furrows surface and then slightly raked to incorporate it to a depth of 2 cm to get a final concentration of 2.4 % of the total dry weight. After the raking, tagged surface of +T furrows was mechanical and statically consolidated using a metal sheet. Ridges were not tagged in any case (Fig. 1a).

It was not possible to measure bulk density when furrows were recently formed because soil was too loose even in furrows with traffic (March 2009). On March 2010 bulk density was considered the same as measured by Boulal et al. (2012) at the top 30 cm because no significant soil condition change was appreciated.

Soil samples from ridges and furrows were taken before and after the rainfall simulations at mini-plot scale from the top 2 cm to measure magnetic susceptibility. Samples from 2 to 6 cm were also taken to ensure that there was no tracer at this depth. Runoff and sediment were collected during the rainfall simulations to determine total runoff, total soil losses and magnetic susceptibility of the sediment.

On July 2009, before the irrigation test at field scale, four furrows (two +T and two –T) were divided in three segments of 5 m length. Three different mixtures of soil and magnetite, hematite and goethite were prepared to get final concentrations, once they were mixed at the field site, of 1.5, 2.5 and 2.5 % of the total dry weight, respectively. These mixtures were spread on the segments surface: magnetite onto the top segments, hematite onto the intermediates and goethite onto the bottom ones (Fig. 1b). A distance of 17.5 m of blank soil was kept among tagged segments. The tagging of soil and application was similar to that made for the small scale rainfall simulations, with the mixture slightly raked to a depth of 2 cm and consolidating soil surface mechanically in trafficked furrows. Ridges were not tagged in any case. A reference furrow without any tracer was also controlled in the irrigation test to analyze the textural class of the sediment collected using the Beckman Coulter LS−230 ®.

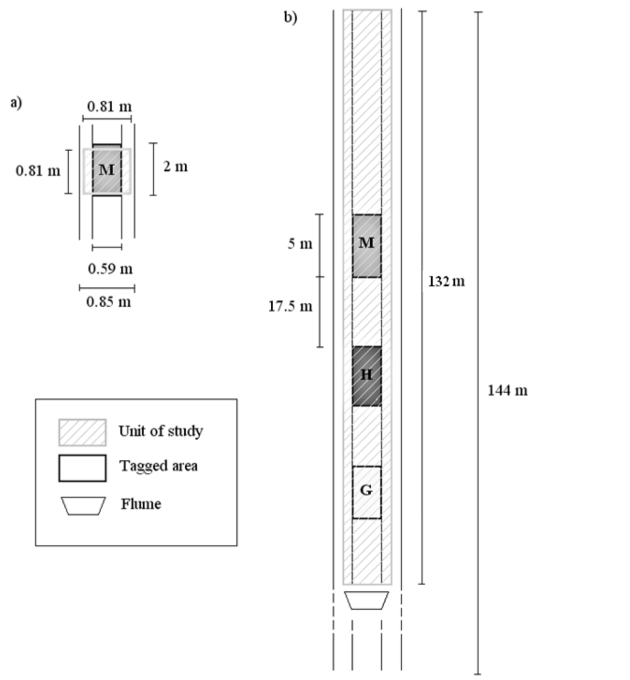

Fig.1. Initial locations of the tagged soil mixture segments with magnetite (M), hematite (H) and goethite (G) on the furrows of small scale (a) and hillslope scale plots (b), (Guzmán, 2012)

Soil samples at two depths (0-2 cm and 2-6 cm) were taken at each tagged area to determine tracer concentration before the irrigation test. After the irrigation, soil samples were taken at the top 2 cm of the profile to determine tracer distributions along each of the eight furrows. Soil samples from 2-6 cm were also taken to ensure that no sediment tracer was at that depth. Each sample was composed by three subsamples taken in the same horizontal transect of the furrow. Location of sampling transects along furrows were 0.5, 2.5 and 4.5 m in tagged segments and 1, 2.5, 5, 10 and 16 m in untagged segments from the beginning of each segment.

Runoff rate was measured and subsamples collected periodically using long-throated flumes of trapezoidal cross section with sill width equal to 100 mm (Clemmens et al. 1984). These flumes were installed 12 m upstream the furrow ends. From the collected runoff, sediment concentration was calculated and total soil losses estimated.

Iron oxide concentrations were analyzed in the recovered sediment through magnetic susceptibility measurements for magnetite and diffuse reflectance spectroscopy for hematite and goethite. The magnitude of the sediment source was determined using tracer concentration in soil and sediment.

The strength of the sediment source was quantified from tracer concentrations in soil and sediment corrected by (i) the distribution of the iron oxides in the soil profile c_d, and (ii) the affinity of the tracers to the finer soil particles c_s (Guzmán, 2012).

2.2.- Soil erosion model

Because of the great width of the ridges surface with respect to the collateral half-ridges, the erosion model of Laguna and Giráldez (1993) was chosen. The model consists of two mass balances, one for sediment and another for water, and one dynamic equation relating water depth and flow rate. The mass balance equation for water, relating the unit flow rate, q, and the water depth, h, to the effective rainfall rate, r_e, gross rainfall, r, minus infiltration rates, i, varying in space, coordinate x, and time, t, is

$$\frac{\partial h}{\partial t}+\frac{\partial q}{\partial x}=r-i=r_e \tag{1}$$

The equation for the mass balance of sediment with a concentration c, includes two terms for the sediment production, one due to the rain splash and other for the runoff shear. Rain splash is represented by a coefficient, B, and an exponent, m, which can assume the value $m=1$. Runoff flow shear has a coefficient, ξ, for the combined effects of aggregates dislodgement, with a coefficient, k, and an exponent b, and of sediment deposition, expressed as the product of sediment concentration by the flow rate

$$\frac{\partial}{\partial t}(hc)+\frac{\partial}{\partial x}(qc)=Br^m+\xi h^b\left(k-\zeta c\right) \tag{2}$$

The equation of the conservation of the momentum for water reduces to a simple potential relationship with the coefficient ς andthe exponent $n=b$

$$q=\zeta h^n \tag{3}$$

Eqs. (1)-(3) were subjected to an initial dry surface condition, $h(x,0)=0$, and a no-flow upstream boundary condition, $h(0,t)=0$, in a surface configuration assimilated to an elongated plane with a width equivalent to the horizontal projection of the half-ridge-furrow-half-ridge ensemble. The system of equations can be solved with the method of characteristics, yielding the solutions for the flow rate, q, depending whether the time was smaller or greater than the concentration time for water, t_{cw}

$$q=\begin{cases} r_e^n t^n & t\le t_{cw}=\left(L\zeta^{-1}r_e^{1-n}\right)^{1/n} \\ r_e L & t>t_{cw}\end{cases} \tag{4}$$

The total length of the plane was L. The solution for the normalized sediment concentration, c^*, using the parameter $k_{B\zeta}=k/(B\zeta)$, is

$$c^*=\frac{c/B-k_{B\zeta}}{1-k_{B\zeta}} \tag{5}$$

with a final expression

$$c^*=\begin{cases} F_n\left[\left(\xi\zeta r^{n-1}n^{-1}\right)^{1/n}t\right] & t\le t_{cw} \\ \left(\xi x\right)^{-1}\left\{1-e^{\mu-\xi x}\left[1-\mu F_n\left(\mu/n\right)\right]\right\} & t_{cw}<t\le t_{cs} \\ F_1\left(\xi x\right) & t>t_{cs}\end{cases} \tag{6}$$

The time for sediment concentration is t_{cs}

$$t_{cs}=\left(\frac{Ln}{\zeta r_e^{n-1}}\right)^{1/n} \tag{7}$$

The function F_n is a generalized version of the Dawson integral (Olver et al. 2010)

$$F_n\left(x\right)=\frac{e^{-x^n}}{x}\int_0^x e^{v^n}\,dv \tag{8}$$

Finally the auxiliary function μ is

$$\mu=\frac{\xi x}{\left(n-1\right)^n}\left\{n-t\left[\frac{\zeta\left(r_e x\right)^{n-1}}{x}\right]^{1/n}\right\}^n \tag{9}$$

Hydrographs and sediment concentrations obtained for each furrow were normalized using the following dimensionless variables

$$t^*=\frac{t-t_{ini}}{t_{eq}-t_{ini}} \tag{10}$$

$$q^* = \frac{q}{q_{eq}} \quad (11)$$

$$c^* = \frac{c}{c_{eq}} \quad (12)$$

Where t_{ini} is time to runoff initiation, t_{eqw} is time to equilibrium for water, t_{eqs} is time to equilibrium for sediments, q_{eq} is equilibrium flow rate and c_{eq} is equilibrium sediment concentration.

To consider the full geometry the distributed model KINEROS2 (Goodrich et al. 2012), a renewed version of KINEROS (Woolhiser et al. 1990), was used.

3.-Results and discussion

On March 2010, bulk densities were assumed to be 1.43 Mg m^{-3} at ridges and 1.52 and 1.47 Mg m^{-3} at +T and −T furrows, respectively (Boulal et al. 2012). Furrow managements at each ridge ground cover show significant differences for runoff when furrows were just formed (Table 1). Due to traffic, soil consolidation was higher in furrows +T than in –T and therefore runoff was higher although soil losses differences were not significant. If furrows were not distinguished according to traffic, significant differences were detected for soil loss when ridges were recently formed and soil was less compacted compared to later in the season (data not shown).

Average runoff was slightly lower on March 2009 (40.9 mm) than on March 2010 (41.3 mm).

Table 1. Average values and standard deviations (in parentheses) for total runoff and soil loss of twelve rainfall simulations at mini-plot scale in furrows with (+T) and without (-T) traffic. $p<0.05$ indicates significant differences between +T and −T furrows grouped by ridge ground covers. A comparison between the two dates was also carried out without distinguishing between +T and −T furrows

		Runoff, mm	Soil loss, kg m^{-2}
Bare	+T	42.3 (0.4)	0.584 (0.089)
(just formed)	–T	39.4 (0.2)	0.658 (0.056)
March 2009	p	0.001	0.289
Standing	+T	39.4 (2.6)	0.313 (0.170)
residues	–T	43.1 (3.2)	0.318 (0.100)
March 2010	p	0.190	0.964
	p	0.782	0.001

Fig. 2 indicates the contribution of each sediment source, ridge or furrow, using magnetic susceptibility measurements. No significant differences were detected between +T and −T furrows in all the cases.

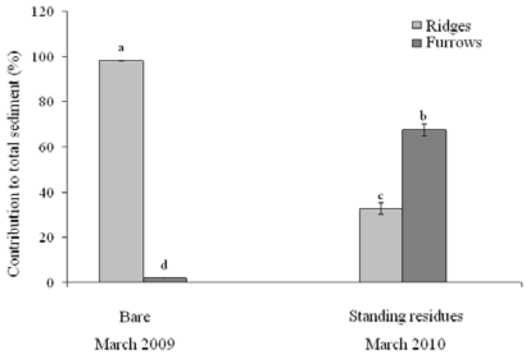

Fig. 2. Average contribution and standard deviation of sediment coming from ridges and furrows distinguishing between bare ridges and ridges with standing residues. Letters indicate significant differences for the different sediment sources at each ridge condition (Bonferroni test $p<0.05$) (Guzmán, 2012)

Table 2 summarizes the key results of the rainfall simulations at field scale. At this scale sediment losses were smaller than the values from the mini-plot scale (0.81 m^2), as a consequence of the lower rainfall rates applied. Ponding time was significantly shorter in the trafficked furrows than in the traffic-free ones. Total runoff and soil loss were lower in the former compared to the latter.

Table 2. Average values and standard deviations (in parentheses) for runoff volume, ponding time, and total soil losses for +T and –T furrows at field scale. $p<0.05$ indicates significant differences between furrows management

Treatment	Runoff, mm	Ponding time, h	Soil loss, kg m^{-2}
+T	59.5 (14.7)	1.93 (0.06)	0.079 (0.018)
–T	25.5 (5.0)	3.93 (0.47)	0.036 (0.008)
p	0.090	0.030	0.220

The analysis of soil samples from the top 2 cm allowed the quantification of the redistribution of tracer after the irrigation, Table 3. No vertical movement was appreciated after the irrigation test. A decreasing trend was observed from the upper segments to the lower ones in both treatments.

Table 3. Average and standard deviation (in parentheses) of tracer concentrations along the top 2 cm of +T and –T furrows after the irrigation test

L, m	Magnetite, %	Hematite, %	Goethite, %
3.0	1.65 (0.39)	-	-
7.5	.030 (0.01)	-	-
11.5	.010 (0.00)	-	-
22.5	.003 (0.00)	-	-
26.5	.005 (0.00)	3.01 (0.75)	-
30.0	.006 (0.00)	.095 (0.00)	-
34.0	.004 (0.00)	.013 (0.01)	-
45.0	.004 (0.00)	.023 (0.00)	-
49.0	.001 (0.00)	.000 (0.10)	2.86 (0.91)
52.5	.002 (0.00)	.033 (0.01)	.038 (0.02)
56.5	.005 (0.00)	.017 (0.01)	.017 (0.01)
67.5	.007 (0.00)	.028 (0.00)	.020 (0.01)

Table 4 presents the estimated values of the model parameters.

Table 4. Estimated values of the erosion model parameters and Nash and Sutcliffe efficiencies of the fits of the model to the experiment data for two of the furrows (+T and −T)

Parameter/Treatment	+T	−T
q_e(mm·h^{-1})	11.7	12.8
c_e(kg·m^{-3})	1.3	1.2
t_{ini}(h)	1.97	5.23
t_{cw}– t_{ini}(h)	2.55	1.37
t_{cs}–t_{ini}(h)	1.72	1.32
n	1.55	1.56
ζ(m^{2-n}·s^{-1})	0.106	0.261
B(kg·m^{-3})	1.80	1.32
k(kg·m^{-1-n}·s^{-1})	0.133	0.293
ξ(m^{-1})	0.129	0.021
e_{NS}	0.879	0.864

The normalized values of runoff and sediment concentration, experimentally obtained, and the prediction of the model, are presented in Fig. 3. The kinematic model shows a typical upwards concavity in the rising hydrograph, (Fig. 3a), as it was already discussed by Woolhiser and Liggett (1967). The sediment concentration tendency, (Fig. 3b), agrees with the predictions of the kinematic wave model, decreasing from the initial values to steadily approach the equilibrium state. This trend is much evident in the furrows + T.

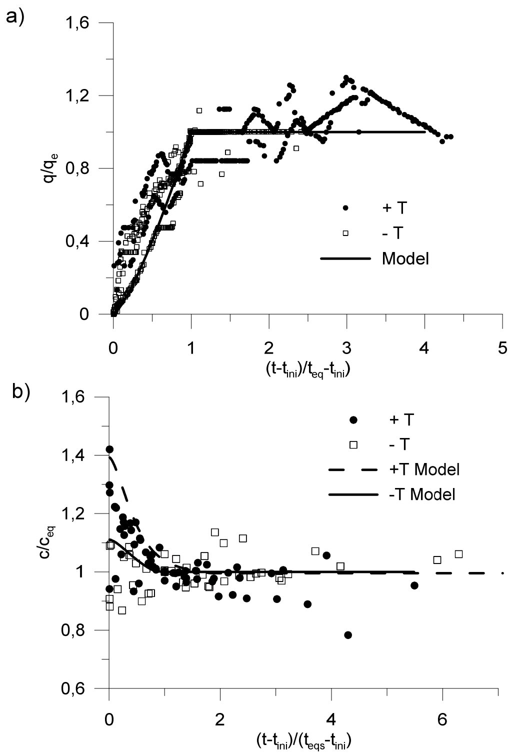

Fig. 3. Normalized hydrograph (a) and sediment concentration evolution (b) for +T and –T furrows. Symbols are experimental data and lines, model prediction

Using the model KINEROS2 based on kinematic wave approximation, the measured hydrographs and sedimentgraphs in each of the furrows were simulated. Figs. 4a,b present the estimated hydrograph and sedimentgraph for one of the furrows of the plot.

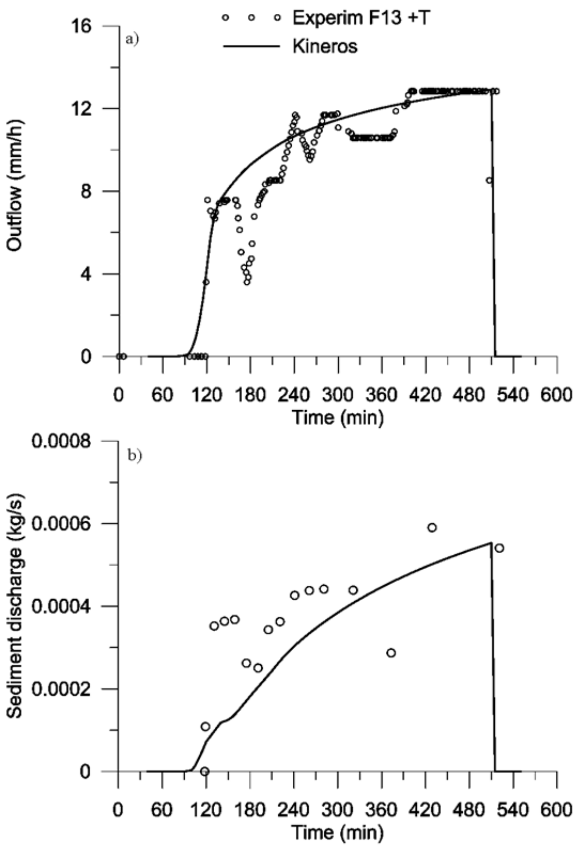

Fig. 4. Measured hydrograph (a) and sedimentgraph (b), open circles, and KINEROS2 simulated curves for the furrow 13 (+T)

The goodness of the fit was estimated with the Nash and Sutcliffe efficiency index. In our case, the worst case was presented by furrow 13 (+T), being the efficiency for its hydrograph and sediment concentration equal to 0.69 and 0.30, respectively (Fig. 4).

KINEROS is initially designed for distributed catchments represented as a cascade of planes and channels. Thus its application to our particular case, the ridge and furrow system, is simplistic as it considers two planes only: the ridge discharging laterally to a channel (the furrow).

To evaluate the sustainability of the system under different situations, several scenarios were generated. In these scenarios the slope of the plot and the length of the furrows were changed maintaining the total water intake of 153 mm and rain intensity. Fig. 5 shows the response of runoff generation and sediment yield combining the variation of slope and length of the +T furrows.

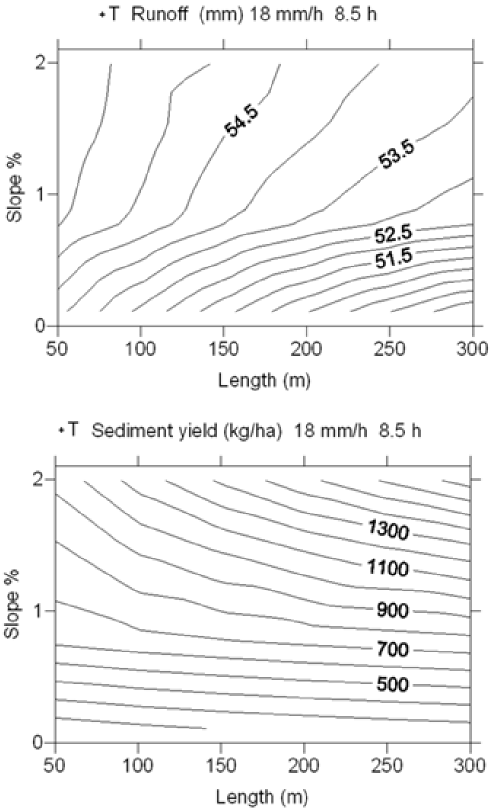

Fig. 5. KINEROS2 simulations of runoff generations and sediment yields for +T furrows varying slope and length conditions for the same rain intensity and duration

The variation of length and slope causes a remarkable response on cumulative runoff and soil losses (Fig. 5), especially when slope increases. For higher slopes and the same conditions, total runoff and soil losses increase significantly. When furrows are longer, soil losses decrease slightly due to the reduction of sediment transport capacity of runoff along the furrows.

4.- Conclusions

There are several key points that must be considered in the selection of iron oxides as sediment tracers, such as their distribution into the soil profile and their selectivity for smaller aggregates. The use of these sediment tracers allowed the: (i) identification of the source of sediments, (ii) quantification of the relative contribution of ridges and furrows, and (iii) monitoring the redistribution of tagged soil along furrows, after the rainfall events and the irrigation test.

Once the crop was standing, furrows and ridges (especially furrows) delivered significantly sediment at the mini-plot scale. At a larger scale an appreciable fraction of sediment coming from tagged furrow was detected in the downstream settling areas. Tagged soil movement followed a decreasing trend as the source was closer to the furrow ends.

This information was also helpful for the calibration of the parameters of the soil erosion model, KINEROS2. Runoff and sediment generation were significantly influenced by length, and especially by slope variations. Further simulations combining these and more factors such as, rainfall intensity and duration, would provide more information about the water erosion processes in these agricultural systems.

In summary, the use of iron oxides (magnetite, hematite and goethite) offers a valuableinformation about water and sediment movement in a ridged system under different crop and traffic conditions. Erosion models are a complementary, powerful tool to understand and to extend the experimental information on soil erosion to different scenarios.

Acknowledgements. This work was funded by the collaborative Project under the 7th EU Framework Research Programme "Compatibility of Agricultural Management Practices and Types of Farming in the EU to enhance Climate Change Mitigation and Soil Health – Catch-C" (Grant Agreement Nr. 289782), Projects AGL2006-10927-C03-01, AGL2006-10927-C03-02 and AGL2009-12936-C03-01 (Spanish Ministry of Science and Innovation), Project P09-AGR-4782 (Consejería de Economía, Innovación y Ciencia of Junta de Andalucía) and FEDER funds.

5.- References

Alves, T., H. Gómez-Macpherson, and J.A. Gómez, 2008.A portable integrated rainfall and overland flow simulator. *Soil Use Manage. 24*, 163-170.

Boulal, H., H. Gómez-Macpherson, J.A. Gómez, and L. Mateos, 2011a. Effect of soil management and traffic on soil erosion in irrigated annual crops. *Soil Till. Res. 115-116*, 62-70.

Boulal, H., L. Mateos, and H. Gómez-Macpherson, 2011b.Soil management and traffic effects on infiltration of irrigation water applied using sprinklers. *Irrig. Sci. 29*, 403-412.

Boulal H., H. Gómez-Macpherson, and F. Villalobos, 2012. Permanent bed planting in irrigated Mediterranean conditions: short-term effects on soil quality, crop yield and water use efficiency. *Field Crops Res.130*, 120-127.

Clemmens, A.J., M.G. Bos, and J.A. Replоge, 1984. Portable RBC flumes for furrows and earthen channels. *Trans. ASAE. 27*, 1016-1022.

Goodrich, D.C., I.S. Burns, C.L. Unkrich, D.J. Semmens, D.P. Guertin, M. Hernandez, S. Yatheendradas, J.R. Kennedy, and L.R. Levick,2012. KINEROS2/AGWA: Model use, calibration, and validation.*Trans. ASABE. 55*, 1561-1574.

Guzmán, G., V. Barrón, and J.A. Gómez, 2010. Evaluation of magnetic iron oxides as sediment tracers in water erosion experiments. *Catena. 82*, 126-133.

Guzmán, M.G., 2012. *Development of sediment tracers to study soil redistribution and sediment dynamic due to water erosion*. Ph.D. diss. Univ. of Cordoba, Dept. of Agronomy.

Guzmán, G., J.N. Quinton, M.A. Nearing, L. Mabit, and J.A. Gómez, 2013.Sediment tracers in water erosion studies: current approaches and challenges. *J. Soil Sediment. 13*,816-833.

Laguna, A., and J.V. Giráldez, 1993. The description of soil erosion through a kinematic wave model. *J. Hydrol. 145*, 65-82.

Llasat, M.C., 2001. An objective classification of rainfall events on the basis of their convective features: application to rainfall intensity in the NE of Spain. *Int. J. Climatol. 21,* 1385-1400.

Mehra, O.P., and M.L. Jackson,1960. Iron oxide removal from soil and clays by a dithionate-citrate system with sodium-bicarbonate buffers. *Clay Clay Miner. 5*, 317-327.

Olver, F.W.J., D.W. Lozier, R.F. Boisvert, and C.W. Clark (Eds.), 2010. *NIST handbook of mathematical functions*. Cambridge Univ. Press.Cambridge.

Soil Survey Staff, 2010. *Keys to soil taxonomy*, 11th ed. USDA-NRCS, Washington, DC, USA.
Strauss, P., G. Guzmán, A. Mentler, R. Hösl, S. Wang, J.A. Gómez, and Z. Zhang, 2012. Evaluation of two sediment tracers under simulated rainfall.Erosion and sediment yields in the changing environment.*IASH Publ. 356*, 327-331.
Walling, D.E., Q. He, and W. Blake, 1999. Use of 7Be and 137Cs measurements to document short- and medium-term rates of water-induced erosion on agricultural land. *Water Resour. Res. 35*, 3865-3874.
Woolhiser, D.A., and J.A. Liggett, 1967. Unsteady, one-dimensional flow over a plane—The rising hydrograph. *Water Resour. Res. 3*, 753-771.
Woolhiser, D.A., R.E. Smith, and D.C. Goodrich, 1990. *KINEROS: a kinematic runoff and erosion model: Documentation and user manual.*US Department of Agriculture, Agricultural Research Service.
Zhang X.C., J.M. Friedrich, M.A. Nearing, and L.D. Norton, 2001. Potential use of rare earth oxides as tracers for soil erosion and aggregation studies. *Soil Sci. Soc. Am. J. 65*, 1508-1515.
Zhang, X.C., M.A. Nearing, V.O. Polyakov, and J.M. Friedrich, 2003. Using rare-earth oxide tracers for studying soil erosion dynamics. *Soil Sci. Soc. Am. J. 67*, 279-288.